Advanced Robotics, Vol. 9, No. 3, pp. 317–329 (1995)

Paper

Investigation of a shape memory alloy actuator for dextrous force-feedback masters

MARWAN A. GHARAYBEH and GRIGORE C. BURDEA

Rutgers, The State University of New Jersey, CAIP Center, CoRE Building, PO Box 1390, Piscataway, NJ 08855-1390, USA

Received for *AR* 16 February 1994; accepted 26 May, 1994

Abstract—Multifingered dextrous robot hands can perform more complex tasks than simpler end effectors. Teleoperation, in which a robot mimics the motion of a remote operator, provides a convenient method for controlling these robot hands. Damage to the object being manipulated by the robot hand may result in the case of open-loop control if there is no force-feedback sensation to the operator from the robot hand. The need arises for new actuator technology to provide force feedback to the hand master. These actuators have to meet the tight space and light weight requirements of a dextrous master. One candidate is the shape memory alloy (SMA) actuator. SMAs, such as Nitinol, are materials with a unique 'mechanical memory' and high force/weight ratio. A prototype SMA actuator and its hardware interface were designed and tested. Results showed that the actuator met the space and weight limitations of the master (Exos DHM^{TM}) and provided adequate reactive force feedback to the operator. However, the actuator had a low bandwidth of operation, due to relatively slow engagement and disengagement motions. This makes it unusable in real-time control situations.

1. INTRODUCTION

Anthropomorphic robotic end effectors such as the Utah/MIT hand [1], the Stanford/JPL hand [2], the Belgrade/USC hand [3] and the NASA hand [4] have been developed to allow increased dexterity in complex robotic tasks.

The autonomous control of robot hands using algorithmic methods is computationally expensive [5] and may be unstable. Teleoperation [6] provides an attractive method for controlling robot hands by utilizing the human hand as the master and the robot hand as the slave. To teleoperate a multifingered robotic end effector, a device must digitize human hand motions. Two commercially available devices that transduce human hand motion are the DataGlove^{TM} [7] and the Exos (Dextrous Hand Master) DHM^{TM} [8]. The DataGlove uses optic fibers stretched over its joints while the DHM is a metallic exoskeleton that uses Hall effect sensors to measure finger

motions. The DHM is considered more accurate than the DataGlove due to better sensors. Both of these masters operate in open loop.

Interaction between the operator and the environment surrounding the robot hand through perceptual sensation of the remote operation process enhances the task performance significantly. Studies done on non-dextrous systems show that task completion times were often reduced by 40% when the operator was given force information [9]. The completion times for the most difficult tasks were reduced by up to 50%.

In considering dextrous masters with force feedback, it is important that they be distinguished from those with tactile feedback. Unlike force feedback, tactile feedback cannot produce rigidity of motion of the operator's hand [10, 11].

A few prototypes of dextrous masters with force feedback have been built such as the Portable Dextrous Master with Force Feedback (PDMFF) [12], the complete hand–arm system built by Jacobsen *et al.* [13] and the master built by Iwata [14]. An ideal force-feedback master should be able to provide the operator with the illusion of 'actually being there', feeling what the robot hand is feeling. Existing masters suffer from one or more problems, such as non-compact non-portable design, restriction to the work volume of the operator's hand [15], inability to provide adequate force to the operator or low bandwidth of operation [10].

Ideal hand masters need to be light and compact to reduce operator fatigue. The requirement for compactness limits the use of cables and pulleys to transmit motion from remotely placed actuators. Therefore, actuators need to be placed on the operator's hand where the forces are to be sensed. This, however, limits the number of degrees of freedom provided with force feedback, because existing actuator technol-

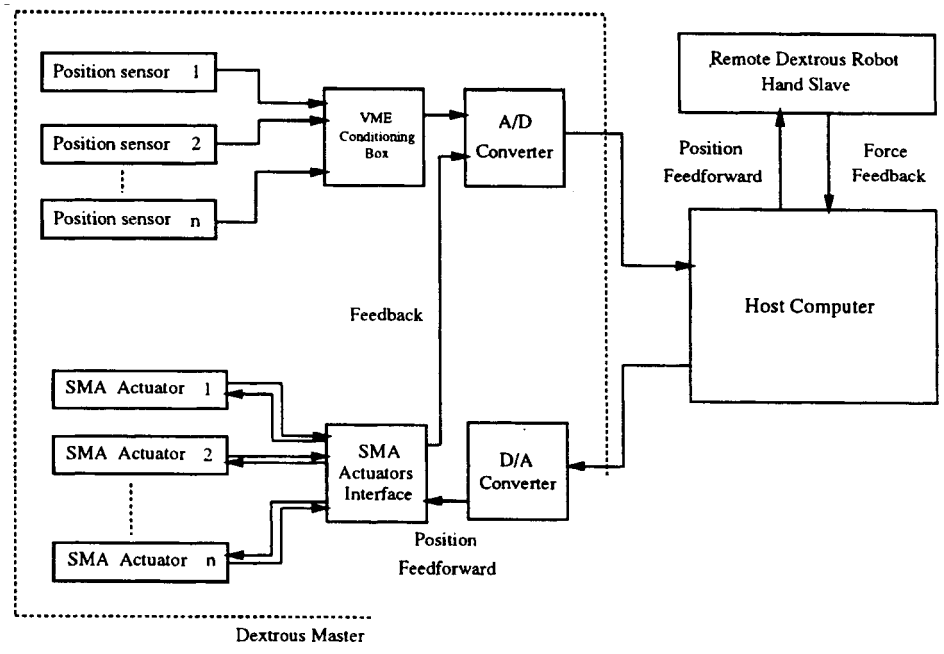

Figure 1. System architecture [20].

ogy has a low power/weight ratio and therefore fewer actuators can be used on the hand to provide force feedback.

To be able to supply multi-d.o.f. force feedback to the DHM, the need arises for new actuator technology that allows more actuators to be placed on the hand. A possible solution in the use of shape memory alloys (SMAs), since they have a high force/weight ratio [16]. SMAs have been used in applications where miniaturization is essential [17, 18]. SMAs are materials with a unique mechanical memory and high force/weight ratio. These materials can memorize a certain 'shape' and can retrieve that particular shape even when deformed. During the process of retrieving their memory shape, SMAs produce large forces that are an order of magnitude larger than those produced by micro-DC motors in the same weight category [16]. SMAs are finding more and more applications into practical actuators, such as in the active medical endoscope [19].

Since heating and cooling of the SMA element must be repeated to operate the actuator, slow cooling rates result in reduced bandwidth of operation for the SMA actuator. This has been a major obstacle towards increased usage of SMA for practical purposes. Several methods have been proposed to increase the bandwidth such as air cooling, water cooling and cooling using a heat sink [18].

Burdea proposed the use of SMAs as the force-feedback actuators for the DHM [20]. The architecture of the proposed system is shown in Fig. 1 [20]. Position sensors on the DHM exoskeleton measure finger link angles, these signals are read by the host computer through an A/D converter and transformed (using calibration software) to finger joint position signals. These data are sent to the dextrous robot hand as position feed-forward signals. The hand responds with force-feedback signals, these signals are decoded and sent to the SMA actuator interface. The interface supplies the necessary current to energize the SMA actuators.

This paper details the design of the SMA actuators and the modification to the structure of the exoskeleton master. Next we present the design of the interface for the SMA actuators. Finally we show how the master is tested using a virtual reality simulation.

2. THE SMA ACTUATOR

Nitinol [21] is the most widely used SMA because of its high repeatability, long life and high power output. If the material is cooled below a certain temperature, called the *martensite* finish temperature, the alloy can be easily deformed permanently (plastically strained). Upon heating above another temperature, called the *austenite* finish temperature, the alloy will attempt to regain the shape it had prior to the deformation. In the process of regaining its original shape the alloy exhibits large forces that can be used for mechanical work. This property is known as the *shape memory effect* (SME). The martensitic transformation from the austenite phase to the martensitic phase starts at a temperature called the martensitic start temperature M_s as shown in Fig. 2. This transformation ends at the martensitic finish temperature M_f, where the specimen is completely transformed into the martensite phase. Due to

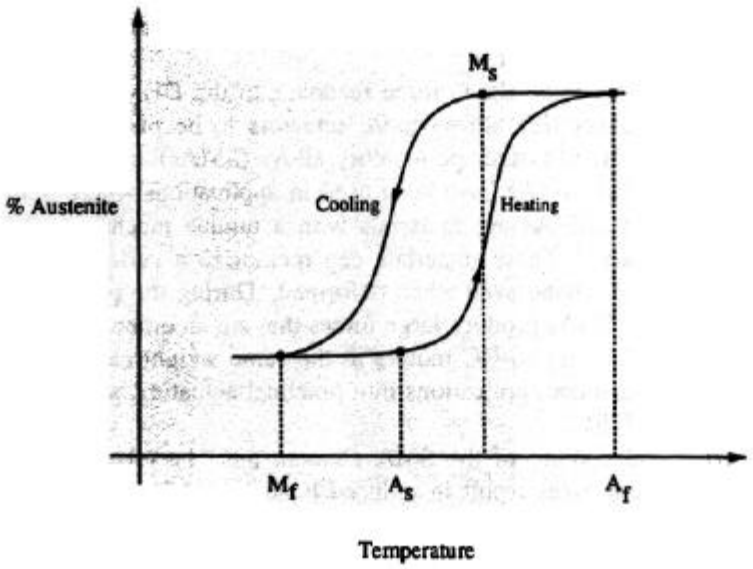

Figure 2. Critical temperatures of martensitic and reverse martensitic transformations.

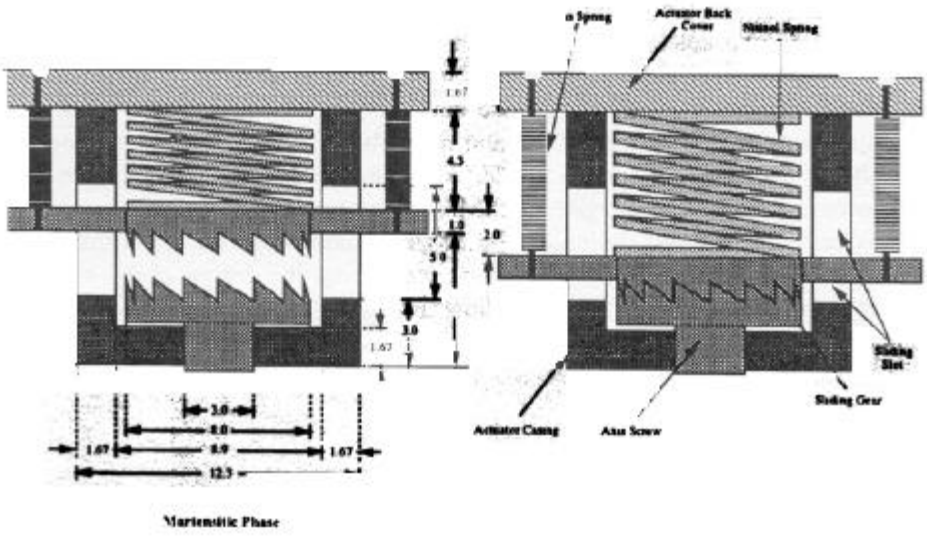

Figure 3. Cross-sectional view of the SMA force-feedback actuator.

hysteresis effects, the reverse martensitic transformation takes place at a different set of temperatures. The evolution of austenite crystals starts at a temperature called the austenitic start temperature A_s and ends at the austenitic finish temperature A_f.

Tests were conducted on several specimens of Nitinol wires, ribbons and springs. It was found that Nitinol springs exhibit much larger strokes as compared with wires and ribbons, but they have smaller electrical resistance and can support smaller loads. Large resistance for a Nitinol element in an SMA actuator is desirable since this

reduces the current requirement and simplifies the design of the interface circuit. Two factors contribute to the resistance of the springs. On one hand, larger loads tend to increase the cross-sectional area and thereafter decrease the resistance. On the other hand, the space compaction produced by the spring windings tend to increase the overall length of the specimen and therefore increase the electrical resistance. The results of these tests showed that Nitinol springs are the most suitable configuration for the proposed force-feedback actuator (due to their large strokes), but at the expense of a more complex driving circuit.

A cross-sectional view into the new actuator design is presented in Fig. 3. The system is composed of the following parts:

(1) *Axis screw.* The axis screw is made out of brass and is fitted with a 16-toothed gear.
(2) *Actuator casing.* The actuator casings is made of transparent plastic. It has a cylindrical groove whose diameter is about 9 mm. The actuator casing comes in two parts to ease the assembly.
(3) *Sliding gear.* This is also a 16-toothed brass gear similar to the gear on the axis screw. The sliding gear has two electrically insulated stop pins on each side. These pins provide space for the bias springs that supply the necessary deformation force for the Nitinol spring. Enough space is available for an electrical connection to the stop pin on the actuator back cover. This gear acts as a heat sink and as an electrode for the Nitinol spring in addition to supplying the necessary reactive force and torque.
(4) *Actuator back cover.* This has two slots where the actuator back screws fit in. It has two pins facing the extension pins on the sliding gear where the bias springs are attached. This piece also acts as a heat sink to the Nitinol spring and as the other electrode for the heating current.
(5) *Actuator back screws.* These screws go through the actuator back cover, the actuator casings and attach to the sensor casing.
(6) *Nitinol spring.* When excited, the Nitinol spring pushes the sliding gear against the gear on the axis screw with sufficient force to make these two gears engage. The force supplied by the Nitinol element overcomes the force supplied by the bias springs and provides the necessary engagement force for the gears. The Nitinol spring has small thickness to increase its resistance and speedup natural cooling.
(7) *Bias springs.* They supply the necessary force to pull the sliding gear to a position where the two gears disengage when the Nitinol spring is cooled to its martensitic phase.

The actuator prototype, shown in Fig. 4, is retrofitted on the Exos Master at the joint where two linkages rotate. On one side of the joint there is the position sensor that senses the operator's finger motion, while on the other side the actuator is installed.

When energized, the actuator blocks the operator's finger flexion towards the palm but it does not restrict its extension away from the palm. This is achieved by the use of one-directional gears such that they slip in one direction, but they block each other's motion in the opposite direction.

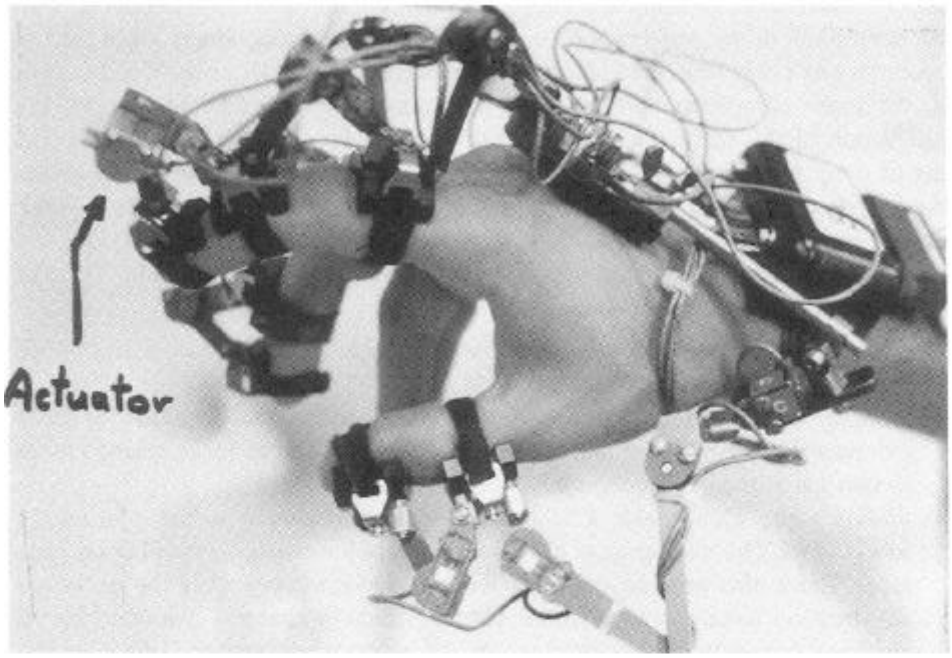

Figure 4. Augmentation to the DHM joint to include the SMA force-feedback actuator.

Table 1.
Data for bandwidth calculation.

Test number	Heating time (s)	Cooling time (s)

The bandwidth of the force-feedback actuator is an important feature. Hogan estimates that the human force compliance control loop has a very low bandwidth of about 1–2 Hz [22]. This represents an upper bound on the required bandwidth of operation for the SMA actuator. The actuator was energized with a step input current of 5.0 A at a duty ratio of 100% and then turned off when the gears engaged. The time needed for the gears to engage and disengage was recorded as shown in Table 1. Using this data, the average bandwidth was calculated at 0.17 Hz. Heating the actuator was responsible for 16% of the average cycle time while cooling was responsible for 84% of this cycle.

The Nitinol spring was in contact with two metallic electrodes, the actuator back cover and the sliding gear. A test was conducted to quantify the effect of these

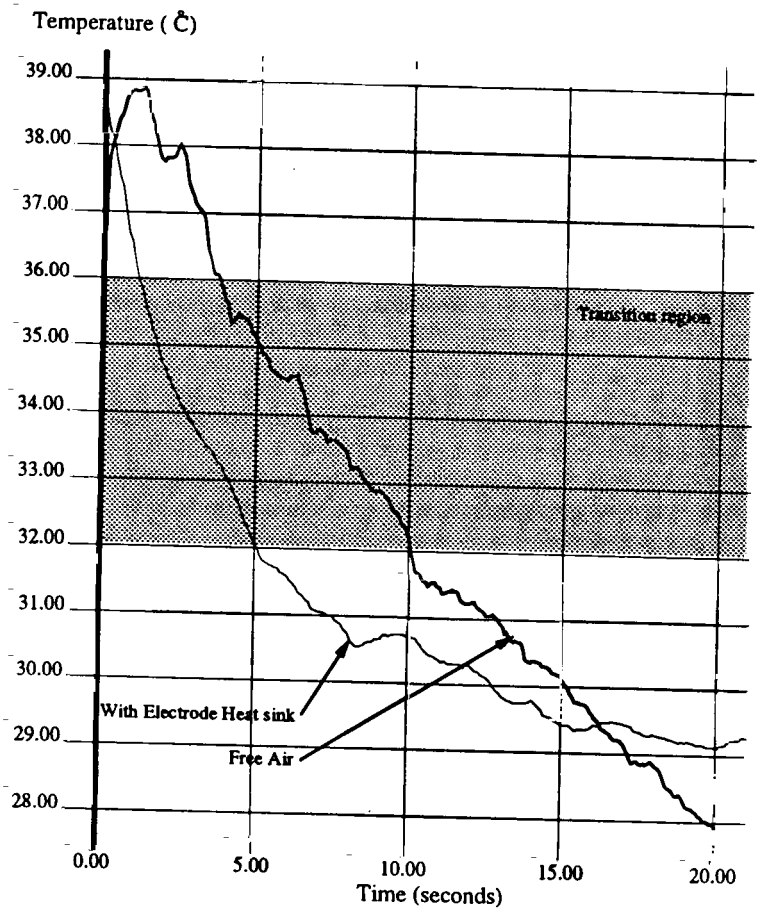

Figure 5. Effect of the electrode heat sink on the cooling rate.

electrodes on the cooling time. A thermocouple was fitted on the spring to measure the temperature while the spring was inside the actuator. The actuator was energized with a DC current to elevate the temperature of the spring to 40°C and allowed to cool while the host computer recorded its temperature. This procedure was repeated with the spring taken out of the actuator and connected directly to the current wires.

Figure 5 shows the results of this experiment. It is noted that the cooling rate of the spring inside the actuator is approximately twice as fast the cooling rate in free air. This is due to the heat sinking effect of the metallic electrodes.

Heating of the actuator could be made arbitrarily higher by the use of a larger power source. However, increasing the cooling rate is more difficult. There are several methods that may be used in the future to increase the cooling rate. For example, Hashimoto *et al.* provided curves for various cooling methods for a 0.8 mm diameter Nitinol wire. The cooling rate when using a heat sink was found to be 30 times faster than that for natural cooling [18]. Cooling via a heat sink is especially convenient for this application since it does not require connection to a central cooling

system. This eliminates the need for pipes or cables to connect to the central unit and therefore does not introduce an extra space requirement.

3. INTERFACE OF THE SMA ACTUATORS

The interface for the SMA actuators was designed to utilize pulse width modulation (PWM) with an amplitude of up to 5.0 A and to provide a visual of the average current flowing into the SMA element. The design is modular and can be expanded for driving up to 16 SMA actuators.

The design of the interface is shown in Fig. 6. The interface with the host computer is through A/D and D/A converters. The signal from the host computer representing the duty cycle is connected to the input of the PWM control circuit. This voltage is in the 0.9–3.5 V range, corresponding to duty ratios of 0–100%, respectively. The output of the PWM control circuit is a low power PWM signal fed to the current chopper

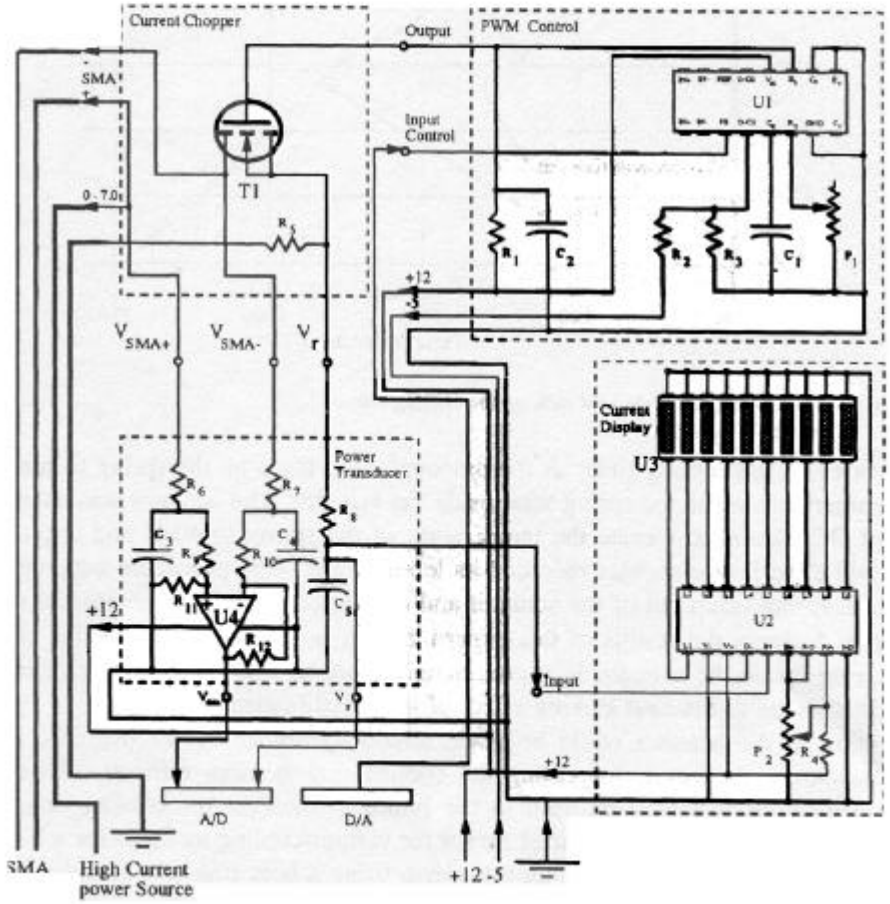

Figure 6. Design of the interface for a single actuator.

circuit at the gate of a high speed MOSFET switch. The current chopper circuit chops a current of amplitude up to 5.0 A at a frequency of 500 Hz. The amplitude of the current chopped by this circuit depends on the voltage setting of a high current power source connected to the circuit. The outputs of this circuit are three signals V_r, V_{SMA+} and V_{SMA-}. These signals are fed to the power transduction circuit. The power transduction circuit feeds back to the host computer two signals proportional to the average current and voltage of the SMA element. The host computer utilizes these two signals to control the SMA actuator. The average current signal is also fed to the current display circuit. The current display circuit is an LED bargraph current meter with a step of 0.5 A.

There are two power supplies for the system. The first is a dual output/low current power supply and the second is a low voltage/high current power supply. The first supply energizes the interface while the second low voltage/high current power source supplies the current needed for heating the SMA actuator.

Figure 7 illustrates the proposed design of the interface for 16 SMA actuators. There are four printed circuit boards, i.e. the PWM control board, the current chopper board, the current transducer board and the bargraph current display board [23]. Each actuator requires connection with one channel of the D/A board and two channels of the A/D board. Thus the total number of channels connected to the interface for 16 SMA actuators is 32 A/D channels and 16 D/A channels.

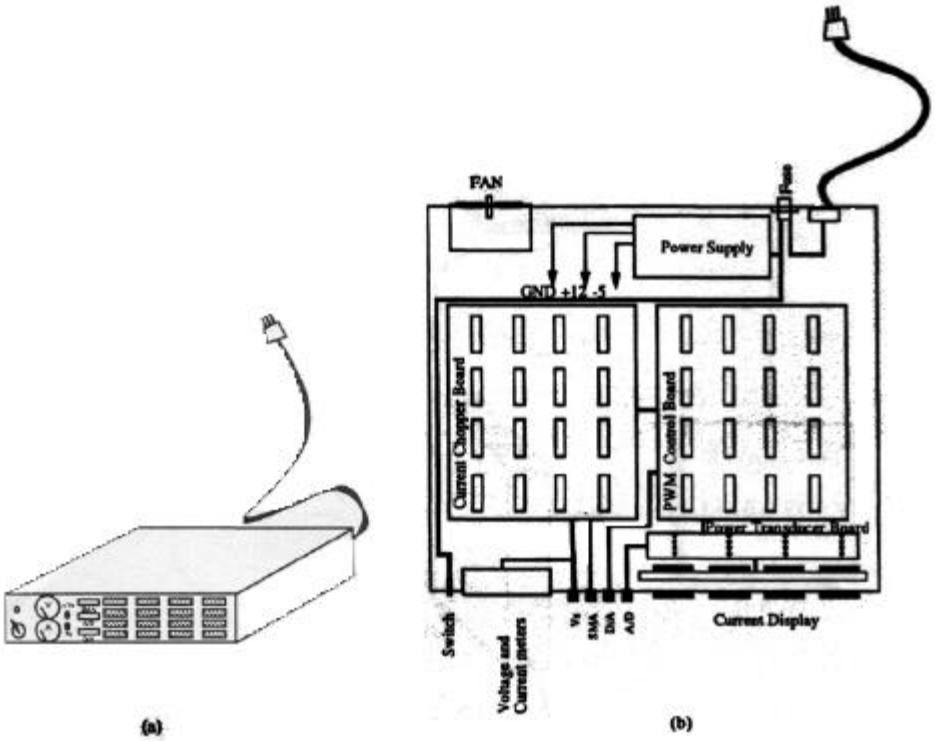

Figure 7. Design of the interface for 16 SMA actuators: (a) overall view and (b) top view.

4. VIRTUAL HAND SIMULATOR

A five fingered virtual robot hand was employed in a world containing virtual objects. Each of its fingers is essentially a 4 d.o.f. robot with three joints just like the human hand. This hand moves in the scene in both rotational and translational motions around three mutually orthogonal axes whose origin is located at the wrist. These motions produce roll, pitch and yaw as well as translation in the x, y and z directions.

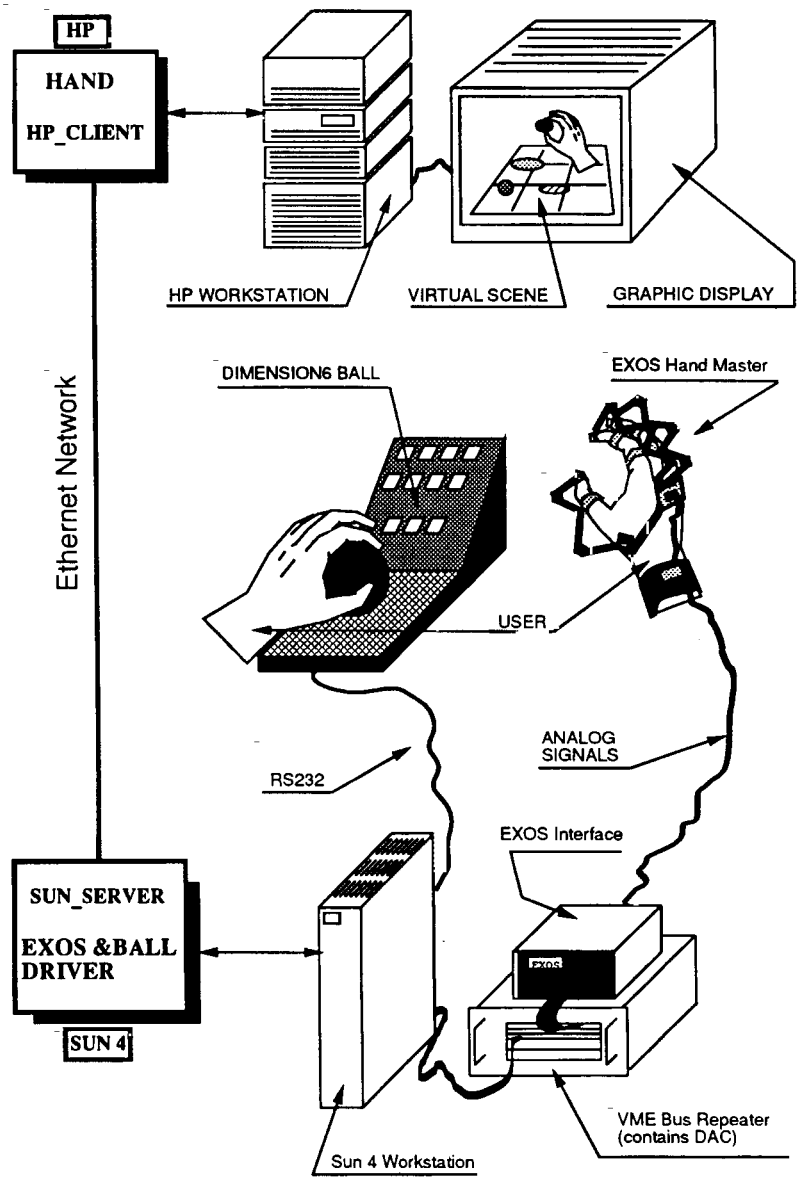

Figure 8. System configuration [24].

The hand interacts with an object in the shape of a ball. A virtual force sensor was installed on the index finger between the MP and PIP joints. As the finger is flexed, it collides with the ball and the virtual force sensor triggers. Subsequently, the SMA force-feedback actuator is energized and the operator 'feels' the interaction with the virtual ball.

The system configuration is shown in Fig. 8 [24]. The dextrous hand simulator is controlled by two devices, the Exos DHM and the Dimension6 Ball Controller [25, 26]. The Dimension6 Ball controller is used to control the position and orientation of the hand wrist in the simulated world, while the DHM controls all finger joint angles.

The simulator utilizes two computers, a SUN 4/360 workstation and an HP 9000/375-SRX Graphics workstation with a 98766 graphics accelerator. The HP displays the virtual hand on the graphics display, while the SUN runs the drivers for the DHM and Dimension6 controllers. The two workstations communicate via the ethernet in a server–client arrangement [12]. On one side of the ethernet the SUN_server reads the shared memory segment that contains the operator's finger joint angles and wrist position and orientations. At the other side, the HP_Client reads the ethernet and stores the received data in a corresponding shared memory segment. A hand simulator uses a simple but realistic model of the human hand. It has a palm and a full set of fingers. Simple objects are also part of the virtual world. A 'display list' technique together with the HP 'Starbase' library [27] enabled the achievment of a graphic refresh rate of up to 10 frames/s for the whole scene.

5. CONCLUSION

In this paper, the process of providing force-feedback sensation for a dextrous master was studied. In addition to applications in telemanipulation, a force-feedback dextrous master is useful in applications such as virtual reality where the operator interacts with virtual objects created by a computer. In such applications, the bandwidth of operation of the force-feedback actuators should be as high as 1–2 Hz or more.

Present actuator technology utilizing electrical solenoids and motors cannot provide actuators with the necessary size and output force. Thus a novel actuator technology is needed. SMAs are materials with high force/weight ratio. Thus they might meet the imposed size requirement.

The SMA actuator was designed and tested. Results of these tests showed that the actuator had a small size of 13 mm, thus it was able to meet the space and weight requirements. The actuators had enough power to supply up to 5.0 N at the midpoint of each finger phalange and thus was able to provide 'near rigidity of motion'. However, it had a relatively low bandwidth of operation of about 0.17 Hz and required a high energizing current of 5.0 A. It is anticipated that even with the rather small bandwidth of operation for the SMA actuators, there would be an improvement in performance with the added force-feedback sensation as opposed to the open-loop performance.

The design of the actuator included metallic electrodes that acts as heat sinks in addition to supplying the necessary energizing current. These electrodes doubled the cooling rate of the Nitinol element.

In the future, a more efficient heat dissipation technique should be utilized to increase the bandwidth of operation of the SMA actuator. This could employ a more efficient heat sink or the use of a forced cooling method such as water cooling that can adhere to the space requirements of the master.

Acknowledgments

The research reported here was supported by National Science Foundation Grant MSS-89-09335, by the CAIP Center, Rutgers University, with funds provided by the New Jersey Commission on Science and Technology and by CAIP's industrial members, and by a Special Purpose Grant from the AT&T Foundation. Special thanks goes to Mr Daniel Gomez for his key contribution in the work on the graphical simulation and to Mr Edward Roskos for his contribution in the ethernet communication part of this project.

REFERENCES

1. S. Jacobsen, E. Iversen, D. Knutti, R. Johnson and K. Biggers, "Design of the Utah/MIT Dextrous Hand," in *Proc. IEEE Conf. Robotics and Automation*, 1986, pp. 1520–1531.
2. J. Salisbury and J. Craig, "Articulated hands: force control and kinematic issues," *Int. J. Robotics Res.*, vol. 1, no. 1, pp. 4–17, 1982.
3. G. Bekey, R. Tomovic and I. Zalikovic, "Control architecture for the Belgrade–USC hand," in *Dextrous Robot Hands*, Locution Publisher, 1990, pp. 136–149.
4. M. S. Ali and J. Charles Engler, "System description document for the Anthrobot-2: a dexterous robot hand," in *NASA Technical Memorandum 104535*, 1991, p. 12.
5. T. H. Speeter, "Transforming human hand motion for telemanipulation," *Presence—Teleoperators and Virtual Environments*, vol. 1, no. 1, pp. 63–79, 1992.
6. T. B. Sheridan, *Telerobotics, automation, and Human Supervisory Control*, Cambridge, MA., 1992.
7. VPL Inc., *DataGlove Operation Manual*, Redwood City, CA, 1987.
8. Exos Inc., *Dexterous Hand Master Users Manual*, Burlingtion, MA, 1990.
9. J. Hill, "Study to design and develop remote manipulator systems", *Technical Report NASA Contract NASA2-8652, SRI Project 4055*, AMES Research Center, Moffett Field, CA, 1976.
10. K. B. Shimoga, "Finger force and touch feedback issues in dextrous telemanipulation," in *Proc. NASA–CIRSSE Int. Conf. Intelligent Robotic Systems for Space Exploration*, 1992.
11. G. Burdea and N. Langrana, "Virtual force feedback: lessons, challeges, future applications," in *ASME Winter Annual Meeting*, 1992.
12. G. Burdea, J. Zhuang, E. Roskos, D. Silver and N. Langrana, "A portable dextrous mater with force feedback," *Presence—Teleoperators and Virtual Environments*, vol. 1, no. 1, pp. 18–27, 1992.
13. S. Jacobsen, E. Iversen, C. Davis, D. Potter and T. McLain, "Design of a multiple degree of freedom, force reflective hand master/slave with a high mobility wrist," in *Third Topical Meeting on Robotics and Remote Systems*, 1989.
14. H. Iwata, "Artificial reality with force-feedback: Development of desktop virtual space with compact master manipulator," *ACM Comp. Graphics*, vol. 24, no. 4, pp. 165–170, 1990.
15. M. Minsky, M. Ouh-young, O. Steele, P. Frederick, J. Brooks and M. Behensky, "Feeling and seeing: issues in force display," *ACM Comp. Graphics*, vol. 24, no. 2, pp. 235–243, 1990.
16. S. Hirose, K. Ikuta and Y. Umetani, "Development of shape-memory alloy actuators. Performance assessment and introduction of a new composing approach," *Adv. Robotics*, vol. 3, no. 1, pp. 3–16, 1989.
17. K. Ikuta, "Application of shape memory actuator for micromechanism," *Precision Eng. Soc. J.*, vol. 54, pp. 1–17, 1988.

18. M. Hashimoto, M. Takeda, H. Sagawa, I. Chiba and K. Sato, "Application of shape memory alloy to robotic actuators," *J. Robotic Syst.*, vol. 2, no. 1, pp. 3–25, 1985.
19. K. Ikuta, M. Tsukamoto and S. Hirose, "Shape memory servo actuator system with electric resistance feedback and application for active endoscope," in *Proc. IEEE*, 1988, pp. 427–430.
20. G. C. Burdea, "Force feedback control for dextrous robot masters using shape memory metals", *National Science Foundation Grant MSS-89-09335*, 1989.
21. W. Buehler and R. Wiley, "Nickel-base alloys", *US Patent: 3,174,851*, 1965.
22. N. Hogan, "Controlling impedance at the man/machine interface," in *Proc. 1989 IEEE Int. Conf. on Robotics and Automation*, 1989, pp. 1626–1631.
23. M. Gharaybeh, "A dextrous hand master with force feedback using shape memory alloy actuators," Master's Thesis, Rutgers University, September 1992.
24. M. Gharaybeh, G. Burdea and D. Gomez, "Teleoperation of a virtual dextrous hand," in *Automatique-Productique Informatique Industrielle*, France, 1992.
25. CIS Graphics, Inc., *Dimension 6 User's Manual*. Westford, 1988.
26. G. Giuliani and G. Burdea, "Telerobotic simulation with the Dimension 6 master on an ardent workstation," *Technical Report CAIP-SR-009*, CAIP Center, Rutgers University, 1990.
27. Hewlett-Packard, *Starbase Graphics Techniques HP-UX Concepts and Tutorials*. Fort Colins, CO, 1988.

ABOUT THE AUTHORS

Marwan **A. Gharaybeh** was born in Amman, Jordan. He received a B.S. and M.S. degrees in Electrical Engineering from the University of Jordan and from Rutgers University in 1988 and 1992, respectively. Currently, Mr. Gharaybeh is pursuing a Ph.D. degree in Electrical Engineering at Rutgers University, USA. His research interests include CAD, virtual reality applications in robotics and process automation.

Dr. Grigore C. Burdea is Associate Professor in the Department of Electrical and Computer Engineering, and Director of the Human-Machine Interface Laboratory of the CAIP Center at Rutgers University. His research focuses on force/tactile feedback for virtual reality and its applications in Medicine. Burdea is author of the book entitled *Virtual Reality Technology* (John Wiley & Sons) and is editor of the book *Computer Integrated Surgery* (MIT Press). He also serves as Associate Editor of the *IEEE Transactions of Robotics and Automation*.